doi: 10.15407/ujpe61.09.0835

V.V. KURYLIUK, S.S. SEMCHUK

Taras Shevchenko National University of Kyiv, Faculty of Physics
(64/13, Volodymyrs'ka Str., Kyiv 01601, Ukraine; e-mail: kuryluk@univ.kiev.ua)

MOLECULAR DYNAMICS CALCULATION OF THERMAL CONDUCTIVITY IN *a*-SiO_2 AND AN *a*-SiO_2-BASED NANOCOMPOSITE

PACS 65.60.+a

Thermal conductivity in amorphous SiO_2 (a-SiO_2) has been studied in a wide range of temperatures, by using the nonequilibrium molecular dynamics method and the Beest–Kramer–Santen, Tersoff, and Vashishta empirical potentials. The thermal conductivity of an a-SiO_2-based composite with Si nanocrystals is calculated with the use of the Tersoff potential. The thermal conductivity of the nanocomposite is shown to firstly decrease and then to increase, as the silicon volumetric ratio grows. The obtained results are explained by the enhanced scattering of thermal vibrations at the matrix–Si nanocrystal boundaries.

K e y w o r d s: thermal conductivity coefficient, molecular dynamics, nanocomposite, amorphous SiO_2, nanocrystal.

1. Introduction

Amorphous silicon dioxide (*a*-SiO_2) is an important material for a number of practical applications owing to some features of its properties, in particular, the weak light absorption in the visible spectral range, chemical inertness, low coefficient of thermal expansion, *etc.* [1]. From the practical viewpoint, the thermal conductivity k is not a less important parameter of *a*-SiO_2. Because of rather a low value of k, *a*-SiO_2 films can be used as thermal barriers at the manufacture of processors and integrated microcircuits. The thermal conductivity in *a*-SiO_2 should be taken into consideration, while studying the thermal properties of graphene layers or carbon nanotubes (in this case, *a*-SiO_2 is used as a thermoinsulating substrate [2, 3]). Recently, composites on the basis of the *a*-SiO_2 matrix with Si or Ge nanocrystals have attracted attention; they are considered as promising materials for the development of novel thermoelectric converters [4–6]. The efficiency of thermoelectric conversion is known to be determined by the formula $ZT = S^2\sigma T/k$, where S is the Seebeck coefficient, σ the electric conductivity, and T the absolute temperature [7]. The insertion of nanocrystals into the *a*-SiO_2 matrix gives rise to a decrease of the thermal conductivity in the material due to the additional scattering of thermal vibrations at interfaces. Therefore, one may expect that the thermoelectric quality factor ZT will grow at that.

The process of heat transfer in amorphous materials also remains to stay in the focus of fundamental science, because the thermal transport in them considerably differs from that in crystalline solids [8]. Several models were proposed for the description of the thermal conductivity in amorphous materials, including *a*-SiO_2, as well as in composite structures on their basis [9–12]. However, relevant calculations do not always agree with experimental data. Either they do not involve the anharmonic coupling between localized vibrational modes, which is one of the main mechanisms of heat transfer in complex compounds of the *a*-SiO_2 type [13], or they require the application of fitting parameters, which points to a necessity of further researches.

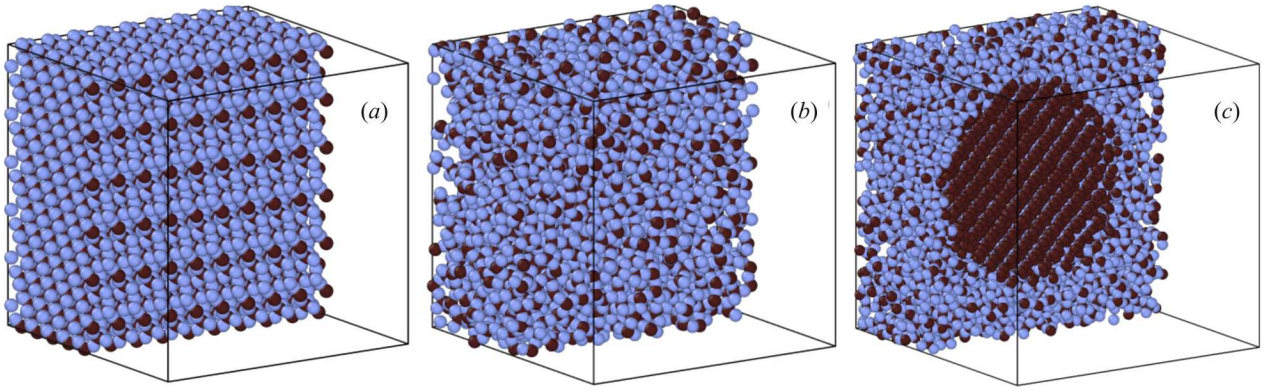

Fig. 1. Cross-section of the studied structure: an initial cell in crystalline α-quartz (a), amorphous SiO_2 after the rapid cooling of a melt (b), the composite structure: the a-SiO_2 matrix and a silicon nanocrystal (c)

The method of molecular dynamics (MD) is regarded to be promising for studying the heat transfer in materials at the atomic level. It has already been applied to simulate the thermal conductivity in a number of crystalline structures and nanocomposites [14–16]. However, the capabilities of this method for calculating the thermal conductivity in amorphous structures, including a-SiO_2, have not been revealed completely. Moreover, one of the problems met by researchers of the thermal conductivity in those materials with the use of the MD method is a proper choice of a potential of the interaction between atoms.

When the structure of amorphous SiO_2 is simulated with the help of the MD technique, the classical Beest–Kramer–Santen (BKS) potential is used as a rule [17]. However, the thermal conductivity of a-SiO_2 calculated with the BKS potential turns out substantially overestimated with respect to experimental data in a wide temperature interval [18,19]. For Si–O-based compounds, Munetoh [20] proposed a parametrization for another known potential, the Tersoff one [21], which had been developed earlier for crystalline Si and Ge. This potential was used to simulate the structure, parameters, and dynamic properties of various SiO_2 modifications, in particular, the lattice parameter, the bound energies, and the density of vibrational states [20]. At the same time, the application of this potential for simulating the heat transfer processes in SiO_2-based structures is reduced to a few works [22].

One more potential of interaction between atoms in the Si–O system was proposed by Vashishta *et al.* [23]. However, the analysis of literature data testifies that the approbation of this model for researches of the thermal conductivity in amorphous SiO_2 was not practically carried out.

In this work, the method of nonequilibrium molecular dynamics was used to calculate the thermal conductivity in amorphous SiO_2 and in a nanocomposite on the basis of a-SiO_2 matrix with Si nanocrystals (Si-nc). The BKS, Tersoff, and Vashishta potentials are tested, while analyzing the thermal conductivity of a-SiO_2 in a wide temperature interval. The Tersoff potential is used to calculate the thermal conductivity in the composite a-SiO_2/Si-nc at $T = 300$ K and various volume fractions of Si nanocrystals.

2. Research Methods

2.1. Structure preparation

In order to study the thermal conductivity in a-SiO_2 and the nanocomposite a-SiO_2/Si-nc, a periodically repeating a-SiO_2 cubic cell with the edge length L_c was generated (Fig. 1). To obtain the cell, we fused crystalline α-quartz (Fig. 1, a) and then annealed it at the temperature $T = 5000$ K for 1 ns until an equilibrium in the liquid phase was attained. The temperature of the system was monitored, by using a Nosé–Hoover thermostat. The obtained melt was cooled down under the constant pressure $P = 0$ at a rate of 10^{11} K/s to a temperature of 300 K, at which the system became thermalized within 1 ns. The resulting structure (Fig. 1, b) was characterized by a disordered arrangement of silicon and oxygen atoms and corresponded to the amorphous phase of the Si–O system.

The nanocomposite structure was created by removing Si and O atoms. A spherical cavity with ra-

dius R was cut out at the a-SiO_2 cell center. The cavity was filled with silicon atoms located at sites of the crystal lattice (Fig. 1, *c*). The relaxation of stresses, which arose when the nanocrystal was inserted, was provided by annealing the structure with the use of the NPT ensemble. Three cells with the edge size $L_c = 5$, 8, or 10 nm were generated. The total number of atoms in the structure varied from 10^4 to 8×10^4. Depending on the ratio between L_c and R, the volume fraction of silicon η changed. It was determined by the formula $\eta = 4\pi R^3/3L_c^3$. The time step in all calculations amounted to 0.5 fs. All MD calculations were carried out with the help of the Large-scale Atomic/Molecular Massively Parallel Simulator (LAMMPS) code [24].

2.2. Potentials of interaction between atoms

2.2.1. Beest–Kramer–Santen (BKS) potential

In the Beest–Kramer–Santen approach, the energy of interaction between atoms i and j is written as follows [16]:

$$E_{ij} = \frac{q_i q_j}{r_{ij}} + A_{ij}\exp(-b_{ij}r_{ij}) - \frac{c_{ij}}{r_{ij}^6}, \tag{1}$$

where q_i is the electric charge of atom i; the constants A_{ij}, b_{ij}, and c_{ij} are determined by the type of interacting atoms; and r_{ij} is the distance between atoms i and j. The parameter values for the BKS potential between atoms in the Si–O-based compounds are quoted in Table 1.

2.2.2. Tersoff potential

In the Tersoff approach, the energy of interaction between atoms is determined by the relation [21]

$$E = \frac{1}{2}\sum_{i\neq j} f_c(r_{ij})[A_{ij}e^{-\lambda_{ij}r_{ij}} - b_{ij}B_{ij}e^{-\mu_{ij}r_{ij}}], \tag{2}$$

where the first and second terms in the brackets describe the interatomic repulsion and attraction, respectively; and the function $f_c(r_{ij})$ is determined as follows:

$$f_c(r_{ij}) = \begin{cases} 1, & r_{ij} < R_{ij}, \\ \dfrac{1}{2} + \dfrac{1}{2}\cos\left[\pi\dfrac{(r_{ij}-R_{ij})}{S_{ij}-R_{ij}}\right], & R_{ij} < r_{ij} < S_{ij}, \\ 0, & r_{ij} > S_{ij}. \end{cases} \tag{3}$$

In Eqs. (2) and (3), all heteropolar interaction constants are calculated using the combination rules: $A_{ij} = (A_i\,A_j)^{1/2}$, $B_{ij} = (B_i\,B_j)^{1/2}$, $R_{ij} = (R_i\,R_j)^{1/2}$, $S_{ij} = (S_i\,S_j)^{1/2}$, $\mu_{ij} = (\mu_i\,\mu_j)^{1/2}$, and $\lambda_{ij} = (\lambda_i\,\lambda_j)^{1/2}$. The term that describes the attraction in Eq. (2) is modulated by the function

$$b_{ij} = \chi_{ij}(1 + \beta_i^{n_i}\zeta_{ij}^{n_i})^{-1/2n_i}. \tag{4}$$

As a result, the force of interaction in every atomic pair becomes dependent on its local environment. The function

$$\zeta_{ij} = \sum_{k\neq i,j} f_c(r_{ik})\omega_{ik}g(\theta_{ijk}), \tag{5}$$

where

$$g(\theta_{ijk}) = 1 + \frac{c_i^2}{d_i^2} - \frac{c_i^2}{d_i^2 + (h_i - \cos\theta_{ijk})^2}, \tag{6}$$

describes the angular dependence of the interaction force. The parameter χ_{ij} characterizes the strength of heteropolar bonds. In particular, for the Si–O system, $\chi_{\text{Si-O}} = 1.17945$. The values of other parameters for the Tersoff potential are quoted in Table 2.

Table 1. **Parameters of the BKS potential for the system Si–O**

i–j	A_{ij}, eV	b_{ij}, Å^{-1}	c_{ij}, eV · Å^6	q_i
O–O	1388.7330	2.76000	175.0000	$q_{\text{O}} = -1.2$
Si–O	18003.7572	4.87318	133.5381	$q_{\text{Si}} = 2.4$

Table 2. **Parameters of the Tersoff potential for the system Si–O**

Parameter	Material	
	Si	O
A, eV	1830.8	1882.55
B, eV	471.18	419.23
λ, Å^{-1}	2.4799	4.17108
μ, Å^{-1}	1.7322	2.35692
β	1.1×10^{-6}	1.1632×10^{-7}
n	0.78734	1.04968
c	1.0039×10^5	1.0643×10^5
d	16.217	4.11127
h	–0.59825	–0.845922
R, Å	2.5	1.7
S, Å	2.8	2

2.2.3. Vashishta potential

To describe the energy of interaction between atoms in Si–O compounds, Vashishta *et al.* proposed a potential which looks like

$$E = \sum_{i<j} V_{ij}^{(2)}(r_{ij}) + \sum_{i,j<k} V_{ijk}^{(3)}(r_{ij}, r_{ik}). \quad (7)$$

Here, $V_{ij}^{(2)}(r_{ij})$ describes the two-particle interaction and is written as follows:

$$V_{ij}^{(2)}(r_{ij}) = \frac{H_{ij}}{r^{\eta_{ij}}} + \frac{Z_i Z_j}{r} - \frac{\alpha_i Z_j^2 + \alpha_j Z_i^2}{2r^4} e^{(-r/r_s)}, \quad (8)$$

where H_{ij} denotes the spatial repulsion force, Z_i the effective charge (in elementary charge units), α_i the electron polarizability of the i-th ion, η_{ij} the repulsion exponent, and r_s the screening length for the dipole interaction. The term $V_{ijk}^{(3)}(r_{ij}, r_{ik})$ makes allowance for the three-particle interaction and is determined as a product of the spatial and angular parts in order to describe the bend and the extension of interatomic bonds:

$$V_{ijk}^{(3)}(r_{ij}, r_{ik}) = R^{(3)}(r_{ij}, r_{ik}) P^{(3)}(\theta_{ijk}), \quad (9)$$

where

$$R^{(3)}(r_{ij}, r_{ik}) = B_{ijk} \exp\left(\frac{l}{r_{ij} - r_0} + \frac{l}{r_{ik} - r_0}\right) \times \Theta(r_0 - r_{ij})\Theta(r_0 - r_{ik}), \quad (10)$$

$$P^{(3)}(\theta_{ijk}) = (\cos\theta_{ijk} - \cos\overline{\theta}_{ijk})^2. \quad (11)$$

In Eqs. (10) and (11), B_{jik} is the strength of the three-particle interaction, θ_{jik} the angle between the vectors $\mathbf{r}_{ji}$ and $\mathbf{r}_{ki}$, and Θ the Heaviside function. The parameter values for the Vashishta potential between atoms in the Si–O system are quoted in Table 3.

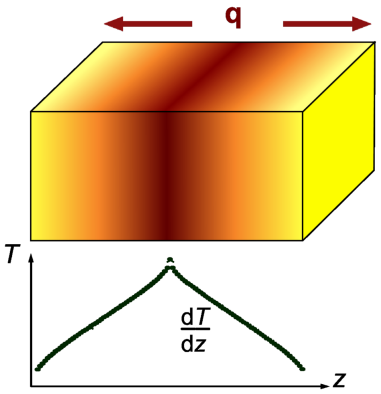

Fig. 2. Schematic diagram of the Müller-Plathe method for the calculation of the thermal conductivity

Table 3. **Parameters of the Vashishta potential for the system Si–O**

i	z	α
Si	1.60	0.00
O	–0.80	2.40
$i-j$	η	H
Si–Si	11	0.057
Si–O	9	11.387
O–O	7	51.692
$i-j-k$	B	$\overline{\theta}$
Si–O–Si	1.40	141.00
O–Si–O	0.35	109.47

2.3. Calculation of the thermal conductivity

The thermal conductivity in amorphous SiO_2 and the composite a-SiO_2/Si-nc was studied within the nonequilibrium molecular dynamics method and the Müller-Plathe algorithm [25]. The principle of the latter is illustrated in Fig. 2. Regions of hot and cold thermostats are created in the simulated specimen. The hot thermostat is located at the center of the specimen, and the cold ones at its ends. A steady thermal flux $\mathbf{q}$ emerges in the specimen, being directed from the hot thermostat in opposite directions, which gives rise to the appearance of the temperature gradient dT/dz. In order to determine the thermal conductivity k in the selected direction z, the researched specimen is divided into $2N$ cells. The central cell (number 1) is considered to be hot, and the end cells (with numbers $\pm N$) to be cold. The thermal flux $\mathbf{q}$ is created owing to the velocity exchange between "hot" atoms in cell 1 and "cold" atoms in cell N. It is determined by the formula

$$q = \sum_{\text{transfers}} \left[\frac{1}{2} M(\nu_h^2 - \nu_c^2)\right] \frac{1}{2tA_c}, \quad (12)$$

where the subscripts "h" and "c" mean "hot" and "cold" atoms, respectively; t is the time interval, during which the energy is transferred; A_c the area of the

transverse cross-section of the structure; and M the atomic mass.

After reaching the stationary state, the temperature of the m-th cell, T_m, is determined by averaging the kinetic energy of n_m atoms in this cell within the time interval t_{av},

$$T_m = \frac{1}{t_{av}} \sum_t \left[\frac{1}{3n_m k_{\rm B}} \sum_{i=1}^{n_m} M_i \nu_i^2(t) \right], \tag{13}$$

where $k_{\rm B}$ is the Boltzmann constant. Knowing the heat flux and the temperature distribution along the direction z, the thermal conductivity k can be determined from the Fourier law:

$$k = -\frac{q}{dT/dz}. \tag{14}$$

In this work, the kinetic energy of atoms in the structure was averaged within 7.5 ns, and every k-value was determined by averaging over five independent simulations.

2.4. Calculation of the density of vibrational states

The density of vibrational states was calculated by applying the Fourier transformation to the velocity autocorrelation function [26]

$$Z(\tau) = \frac{\langle \mathbf{v}(\tau)\mathbf{v}(\theta) \rangle}{\langle \mathbf{v}(0)\mathbf{v}(0) \rangle}, \tag{15}$$

where $\mathbf{v}(0)$ and $\mathbf{v}(\tau)$ are the particle velocity vectors at the time moments $t = 0$ and τ, respectively. The averaging in Eq. (15) was carried out for all particles at $T = 300$ K and within $\tau = 50$ ps. The density of vibrational states was calculated as a quantity that is proportional to the Fourier transform of the Z-function averaged over all particles:

$$n(\omega) \sim \int_{-\infty}^{\infty} Z(\tau) e^{i\omega\tau} d\tau. \tag{16}$$

3. Results and Their Discussion

The value of thermal conductivity calculated within the Müller–Plathe method is known to be sensitive to the cell size L_c:

$$\frac{1}{k_0} = \frac{1}{k} + \frac{\alpha}{L_c}, \tag{17}$$

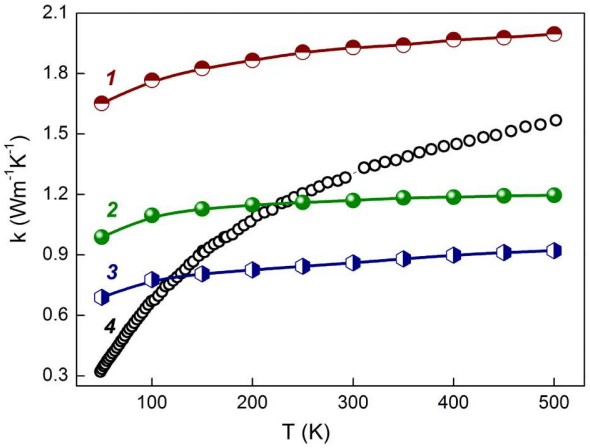

Fig. 3. Temperature dependences of the thermal conductivity in a-SiO_2 calculated, by using the BKS (*1*), Tersoff (*2*), and Vashishta (*3*) potentials. Curve *4* corresponds to the experimental dependence $k(T)$ obtained according to the data of work [27]

where k_0 is the thermal conductivity calculated for a cell with the size L_c, k the value extrapolated to the case of bulk material ($L_c \to \infty$), and the coefficient α does not depend on L_c. Therefore, the thermal conductivity for bulk a-SiO_2 was determined by preliminarily plotting the dependences of the reciprocal thermal conductivity $1/k_0$ on the reciprocal length $1/L_c$, which were then extrapolated to $L_c \to \infty$. In Fig. 3, the results of MD calculations of the temperature dependence of the thermal conductivity for a-SiO_2 with the use of the described technique with engaging all three potentials of interaction between atoms are shown (curves *1–3*). For comparison, the experimental dependence $k(T)$ obtained in work [27] is also depicted (curve *4*).

From the presented data, it follows that the MD simulation with the BKS potential gives overestimated values for the thermal conductivity of a-SiO_2 in the whole researched temperature interval. In the low-temperature section ($T \sim 50$ K), the theoretical k-values exceed the experimental ones by almost a factor of 5. As the temperature grows, this discrepancy gradually decreases to approximately 30% at $T \sim 500$ K. This result agrees with the data obtained by other authors [18,19] and demonstrates the limited capabilities of the BKS potential for the calculation of the thermal conductivity in a-SiO_2.

The MD simulation with the Tersoff potential also gives rise to deviations of the theoretical depen-

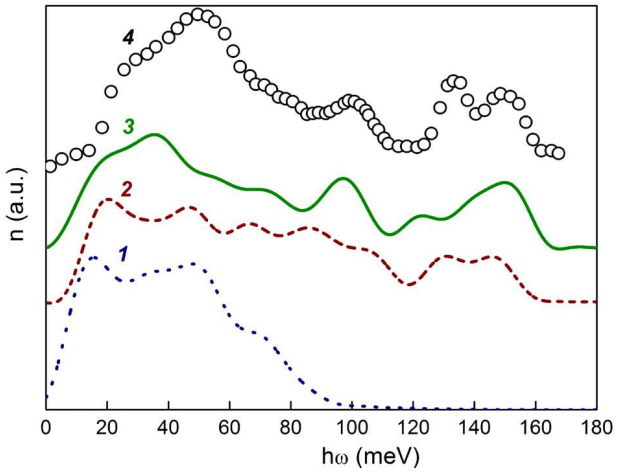

Fig. 4. Density of vibrational states in a-SiO_2 calculated with the use of the Vashishta (*1*), BKS (*2*), and Tersoff (*3*) potentials. Curve *4* corresponds to the experimental dependence $n(\hbar\omega)$ obtained according to the data of work [28]

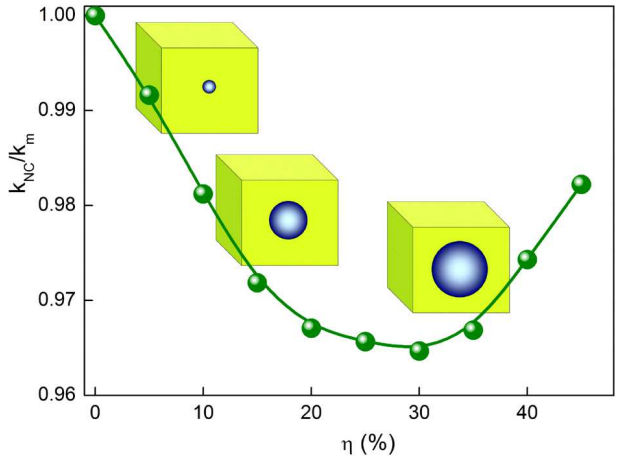

Fig. 5. Relative thermal conductivity of the nanocomposite a-SiO_2/Si-nc as a function of the volume fraction of silicon

dence $k(T)$ from the experimental one. In the low-temperature section, the theoretical k-values turn out overestimated with respect to the experiment by approximately a factor of two. As the temperature grows, the inverse relationship is established so that, at $T \sim 500$ K, the theoretical k-values are smaller than the experimental ones by 25%. Moreover, the thermal conductivity calculated with the Tersoff potential grows more slowly with the temperature than the experimental curve $k(T)$.

The application of the Vashishta potential for the calculation of the thermal conductivity in a-SiO_2 results in considerably underestimated values in a wide temperature interval. The corresponding theoretical dependence $k(T)$ demonstrates a weak variation of k with the temperature. In particular, in the interval $T = 50 \div 500$ K, the value of k changes from 0.69 to 0.92 W/(m K), whereas the experimental data vary from 0.32 to 1.56 W/(m K).

Hence, of three studied potentials for the interaction between atoms, the Tersoff potential brings about the k-value for a-SiO_2 at room temperature that is the closest to the experimental one, k_{exp}; namely, $k = 1.17$ W/(m K), which is only 11% lower than k_{exp}. The corresponding values of k calculated in the framework of the MD method with the BKS and Vashishta potentials amount to 1.93 and 0.86 W/(m K), respectively. The mismatch between the experimental and calculated dependences $k(T)$ for amorphous SiO_2 has several origins. First, the temperature dependence of the thermal conductivity in solids at low temperatures is known to be determined by the behavior of the heat capacity C_v. The latter parameter drastically diminishes as the temperature decreases [8]. In classical molecular dynamics, the value of C_v is a temperature-independent constant (the Dulong–Petit law). Therefore, the k-values calculated at low temperatures will be overestimated with respect to the experimental data irrespective of the chosen potential. Second, the mismatch of theoretical and experimental k-values is also associated with shortcomings in the parametrization of the potentials of atom-to-atom interaction selected for the calculation of the thermal conductivity in the amorphous phase of the Si–O system.

The density of vibrational states, $n(\omega)$, is an important characteristic of the thermal motion of atoms in solids. It was calculated following the technique that was described in Section 2. Figure 4 illustrates the results of MD calculations of the dependence $n(\omega)$ at $T = 300$ K obtained for the potentials of interatomic interaction described above (curves *1–3*) and the experimental dependence adapted from work [28] (curve *4*). It is known that three bands – in vicinities of 40, 100, and 130–150 meV – are distinguished in the spectrum of vibrational states in amorphous silicon dioxide. They are associated with the torsional, bending, and stretching-compression, respectively, vibrations of Si–O–Si bonds. The results obtained (Fig. 4) testify that the potentials of interaction between atoms, which were used in this

work, bring about considerably different $n(\omega)$ spectra. In particular, the dependence $n(\omega)$ calculated with the use of the Vashishta potential is characterized by the absence of high-frequency bands that correspond to the bending and stretching-compression vibrations. On the other hand, the application of the BKS potential practically does not allow the bands associated with the torsional and bending vibrations to be resolved. At the same time, the calculations with the Tersoff potential satisfactorily reproduce both the structure of the experimental dependence $n(\omega)$ and the frequency positions of separate bands.

Taking those facts into account, the Tersoff potential was chosen for further calculations of the thermal conductivity in the nanocomposite on the basis of the a-SiO_2 matrix with a spherical silicon nanocrystal. We studied the relative change of the thermal conductivity in this material, $k_{\rm NC}/k_m$ ($k_{\rm NC}$ and k_m are the thermal conductivity in the structure with Si nanoinclusions and in the pure a-SiO_2 matrix, respectively), as a function of the volume fraction of silicon nanocrystals, η, which was changed by choosing the corresponding radius of nanocrystals. The temperature was selected to be $T = 300$ K. From the results of calculations that are presented in Fig. 5, one can see that if the fraction of silicon nanocrystals increases, the thermal conductivity in the nanocomposite smoothly decreases at first, passes through a minimum at some threshold value $\eta_{\rm th}$, and then grows. In our opinion, such a behavior of the dependence $k(\eta)$ is a result of two competing factors. On the one hand, the increase of the silicon fraction should stimulate a permanent growth of the thermal conductivity in the nanocomposite, because the thermal conductivity of Si is higher in comparison with that in the a-SiO_2 matrix material. But on the other hand, the growth of η and, accordingly, the radius of Si nanocrystals is accompanied by the growth of the area of the matrix/nanocrystal boundary, at which thermal vibrations are scattered. The latter process stimulates a reduction of the thermal conductivity. Therefore, the recession in the dependence $k(\eta)$ at $\eta < \eta_{\rm th}$ can be explained by the dominant role of the scattering of thermal vibrations by the nanocrystal boundaries. At the same time, the growth of k at $\eta > \eta_{\rm th}$ is governed by a high content of the thermal-conducting material (silicon). This result demonstrates a possibility to vary the thermal conductivity in the nanocomposite material a-SiO_2/Si-nc, which may form a basis for the development of thermoelectric converters.

4. Conclusions

In this work, using the method of nonequilibrium molecular dynamics, the temperature dependence of the thermal conductivity k in amorphous SiO_2 was calculated, with engaging the empirical Beest–Kramer–Santen, Tersoff, and Vashishta potentials for the interaction between atoms. In the interval of room temperatures, the Tersoff potential was found to give the k-value that is the closest to experimental data and better reproduces the spectrum of vibrational modes in a-SiO_2. The Tersoff potential was used to simulate the change of the thermal conductivity in a composite material on the basis of a a-SiO_2 matrix with Si nanoinclusions as a function of the volume fraction η of silicon, $k(\eta)$. The results obtained were explained by the action of two competing factors: 1) the increase of the area of nanocrystal boundaries, which manifests itself in a reduction of the dependence $k(\eta)$ at low η; and 2) the increase of the fraction of the material with a high thermal conductivity (Si), which gives rise to the growth of k at η above a certain threshold value $\eta_{\rm th}$.

The authors express their gratitude to M.M. Bogolyubov Institute for Theoretical Physics of the NAS of Ukraine for the access to the Grid computer cluster used in calculations by the molecular dynamics method.

1. *Silica: Physical Behavior, Geochemistry, and Materials Applications. Series: Reviews in Mineralogy, Vol. 29*, edited by P.J. Heaney, C.T. Prewitt, and G.V. Gibbs (Mineral. Soc. of America, 1994).
2. A.A. Balandin, Thermal properties of graphene and nanostructured carbon materials, *Nat. Mater.* **10**, 569 (2011) [DOI: 10.1038/nmat3064].
3. Z.-Y. Ong and E. Pop, Molecular dynamics simulation of thermal boundary conductance between carbon nanotubes and SiO_2, *Phys. Rev. B* **81**, 155408 (2010) [DOI: 10.1103/PhysRevB.81.155408].
4. H.-T. Chang, C.-C. Wang, J.-C. Hsu, M.-T. Hung, P.-W. Li, and S.-W. Lee, High quality multifold Ge/Si/Ge composite quantum dots for thermoelectric materials, *Appl. Phys. Lett.* **102**, 101902 (2013) [DOI: 10.1063/1.4794943].
5. O. Korotchenkov, A. Nadtochiy, V. Kuryliuk, C.-C. Wang, P.-W. Li, and A. Cantarero, Thermoelectric energy conversion in layered structures with strained Ge quantum dots

grown on Si surfaces, *Eur. Phys. J. B* **87**, 64 (2014) [DOI: 10.1140/epjb/e2014-50074-8].
6. H.-T. Chang, S.-Y. Wang, and S. Wei, Designer Ge/Si composite quantum dots with enhanced thermoelectric properties Nanoscale **6**, 3593 (2014) [DOI: 10.1039/c3nr06335f].
7. A. Majumdar, Thermoelectricity in semiconductor nanostructures, Science **303**, 777 (2004) [DOI: 10.1126/science.1093164].
8. R.C. Zeller and R.O. Pohl, Thermal conductivity and specific heat of noncrystalline solids, *Phys. Rev. B* **4**, 2029 (1971) [DOI: 10.1103/PhysRevB.4.2029].
9. J.J. Freeman and A.C. Anderson, Thermal conductivity of amorphous solids, *Phys. Rev. B* **34**, 5684 (1986) [DOI: 10.1103/PhysRevB.34.5684].
10. P.B. Allen and J.L. Feldman, Thermal conductivity of glasses: theory and application to amorphous Si, *Phys. Rev. B* **62**, 645 (1989) [DOI: 10.1103/PhysRevLett.62.645].
11. P.B. Allen, J.L. Feldman, J. Fabian, and F. Wooten, Diffusons, locons and propagons: Character of atomic vibrations in amorphous Si, *Philos. Mag. B* **79**, 1715 (1999) [DOI: 10.1080/13642819908223054].
12. V. Kuryliuk, A. Nadtochiy, O. Korotchenkov, C.-C. Wang, and P.-W. Li, A model for predicting the thermal conductivity of SiO_2/Ge nanoparticle composites, *Phys. Chem. Chem. Phys.* **17**, 13429 (2015) [DOI: 10.1039/C5CP00129C].
13. S. Shenogin, A. Bodapati, P. Keblinski, and A.J.H. McGaughey, Predicting the thermal conductivity of inorganic and polymeric glasses: The role of anharmonicity, *J. Appl. Phys.* **105**, 034906 (2009) [DOI: 10.1063/1.3073954].
14. X. Li and R. Yang, Equilibrium molecular dynamics simulations for the thermal conductivity of Si/Ge nanocomposites, *J. Appl.* Phys. **113**, 104306 (2013) [DOI: 10.1063/1.4794815].
15. J.B. Haskins, A. Kinaci, and T. Cagin, Thermal conductivity of Si-Ge quantum dot superlattices, Nanotechnology **22**, 155701 (2011) [DOI: 10.1088/0957-4484/22/15/155701].
16. M.-J. Huang and T.-M. Chang, Thermal transport within quantum-dot nanostructured semiconductors, *Int. J. Heat Mass Tran.* **55**, 2800 (2012) [DOI: 10.1016/j.ijheatmasstransfer.2012.02.001].
17. B.W.H. van Beest, G.J. Kramer, and R.A. van Santen, Force fields for silicas and aluminophosphates based on ab initio calculations, *Phys. Rev. Lett.* **64**, 1955 (1990) [DOI: 10.1103/PhysRevLett.64.1955].
18. P. Jund and R. Jullien, Molecular-dynamics calculation of the thermal conductivity of vitreous silica, *Phys. Rev. B* **59**, 13707 (1999) [DOI: 10.1103/PhysRevB.59.13707].
19. A.J.H. McGaughey and M. Kaviany, Thermal conductivity decomposition and analysis using molecular dynamics simulations: Part II. Complex silica structures, *Int. J. Heat Mass Tran.* **47**, 1799 (2004) [DOI: 10.1016/j.ijheatmasstransfer.2003.11.009].
20. S. Munetoh, T. Motooka, K. Moriguchi, and A. Shintani, Interatomic potential for Si-O systems using Tersoff parameterization, *Comput. Mater. Sci.* **39**, 334 (2007) [DOI: 10.1016/j.commatsci.2006.06.010].
21. J. Tersoff, Modeling solid-state chemistry: Interatomic potentials for multicomponent systems, *Phys. Rev. B* **39**, 5566 (1989) [DOI: 10.1103/PhysRevB.39.5566].
22. J. Yeo, Z.S. Liu, and T.Y. Ng, Enhanced thermal characterization of silica aerogels through molecular dynamics simulation, *Model. Simul. Mater. Sci. Eng.* **21**, 075004 (2013) [DOI: 10.1088/0965-0393/21/7/075004].
23. P. Vashishta, R.K. Kalia, J.P. Rino, and I. Ebbsjo, Interaction potential for SiO_2: A molecular-dynamics study of structural correlations, *Phys. Rev. B* **41**, 12197 (1990) [DOI: 10.1103/PhysRevB.41.12197].
24. S. Plimpton, Fast parallel algorithms for short-range molecular dynamics, *J. Comp. Phys.* **117**, 1 (1995) [DOI: 10.1006/jcph.1995.1039].
25. F. Müller-Plathe, A simple nonequilibrium molecular dynamics method for calculating the thermal conductivity, *J. Chem. Phys.* **106**, 608 (1997) [DOI: 10.1063/1.473271].
26. C.Z. Wang, C.T. Chan, and K.M. Ho, Tight-binding molecular-dynamics study of phonon anharmonic effects in silicon and diamond, *Phys. Rev. B* **42**, 11276 (1990) [DOI: 10.1103/PhysRevB.42.11276].
27. D.G. Cahill, Thermal conductivity measurement from 30 to 750 K: the 3w method, *Rev. Sci. Instrum.* **61**, 802 (1990) [DOI: 10.1063/1.1141498].
28. J.M. Carpenter and D.L. Price, Correlated motions in glasses studied by coherent inelastic neutron scattering, *Phys. Rev. Lett.* **54**, 441 (1985) [DOI: 10.1103/PhysRevLett.54.441].

Received 10.04.16.
Translated from Ukrainian by O.I. Voitenko

В.В. Курилюк, С.С. Семчук

РОЗРАХУНОК ТЕПЛОПРОВІДНОСТІ a-SiO_2 ТА НАНОКОМПОЗИТА НА ЙОГО ОСНОВІ МЕТОДОМ МОЛЕКУЛЯРНОЇ ДИНАМІКИ

Р е з ю м е

За допомогою методу нерівноважної молекулярної динаміки розраховано теплопровідність аморфного SiO_2 в широкому інтервалі температур з використанням емпіричних потенціалів міжатомної взаємодії Біста–Крамера–Сентена, Терсоффа та Вашишти. З використанням потенціалу Терсоффа розраховано теплопровідність композита на основі аморфного SiO_2 з нанокристалами Si. Показано, що зі збільшенням об'ємної частки кремнієвих нанокристалів теплопровідність нанокомпозита спочатку зменшується, досягає мінімуму і починає поступово зростати. Отримані результати пояснено з точки зору розсіювання теплових коливань на межах поділу матриця–нанокристал.